Theory of the angle-dependent autoionization cross section in ion-atom collisions

Ivan L. Cordrey and Joseph H. Macek
Department of Physics and Astronomy, University of Tennessee, Knoxville, Tennessee 37996
and Oak Ridge National Laboratory, Oak Ridge, Tennessee 37831
(Received 5 February 1993)

The angle-dependent cross section for perturbed overlapping autoionization lines excited in ion-atom collisions is derived analytically. This electron angular distribution shows strong enhancement in the forward direction, and includes interference between overlapping lines that profoundly affect the cross section in the forward direction. The relative cross sections of autoionization lines excited in He^+ + He collisions at 5, 10, and 15 keV are calculated and found to be in good agreement with experiment.

PACS number(s): 34.50.Fa

I. INTRODUCTION

In low-velocity ion-atom collisions where a projectile ion P^{Z+} collides with a target T leaving it in an autoionizing state T^{**} that decays in the presence of the moving projectile, shown schematically by

$$P^{Z+} + T \rightarrow P^{Z+} + T^{**} \rightarrow P^{Z+} + e^- + T^+, \quad (1.1)$$

the autoionized electron interacts with both the projectile and the target in the final state, an effect that is called post-collision interaction (PCI) [1–6].

Miraglia and Macek [7] divide PCI into three basic effects: binding, focusing, and Stark mixing. "Binding" describes the shift in energy of the autoionization electron due to changes in its binding energy caused by the potential well of the charged projectile. The binding effect changes the unperturbed autoionization Lorentzian line shape into an asymmetrically broadened line shape with a low-energy tail. This effect has received the most attention, and is incorporated in many formulas for autoionization electron energy distribution. Barker and Berry [3] include this binding-energy shift phenomenologically. Devdariani, Ostrovsky, and Sebyakin [4] derive the line shape using a quantum-mechanical resonance model coupled to the electron continuum in the presence of the projectile's Coulomb potential. Van der Straten and Morgenstern [5] use a semiclassical model to account for the effect of the projectile's potential. "Focusing," or Coulomb focusing, describes the alteration of the electron's angular distribution due to the presence of the projectile in the final state. Coulomb focusing modifies the autoionization cross section yielding strong enhancement in the forward direction. This effect also modifies the line shape of an isolated line due to the interference of the direct and scattered components of the final-state wave function of a single autoionized electron state. Coulomb focusing is incorporated into two quantal theories [2, 8], which also include the binding effects. Barrachina and Macek [8] use an approach similar to Devdariani, Ostrovsky, and Sebyakin's approach, but include the presence of the projectile in the final state explicitly by using the continuum distorted-wave wave function for the final-state wave function. Kuchiev and Sheinerman [2] use an alternative quantum-mechanical final state applicable to electron excitation and heavy-ion excitation. For heavy-ion collisions where the projectile ion follows a semiclassical trajectory, these two theories are equivalent. There is also a semiclassical electron-trajectory model of focusing presented by Swenson and co-workers [9, 10]. "Stark mixing" describes the changes in autoionizing state populations (particularly for states close in resonant energy) that occur in the excited state T^{**} due to the projectile's electric field. Stark mixing has its greatest effect in the tail of the line shape, which corresponds to small internuclear separation of target and projectile. It changes the state populations, and significantly affects the phase of the autoionization amplitude. Stark mixing is discussed by Stolterfoth, Brand, and Prost [6], and by Miraglia and Macek [7], who extended the work of Ref. [8] to include Stark mixing.

The work reported here uses the binding-shifted, Coulomb-focused, and Stark-mixed autoionization amplitude of Miraglia and Macek [7] to derive an analytical expression for the angle-dependent autoionization transition probability (which is proportional to the cross section) for perturbed overlapping lines. With overlapping lines, the interference between different lines can significantly alter the qualitative features of the full autoionization electron spectrum and, as will be shown, this interference can also affect the angle-dependent cross section. This work differs from the calculation of Ref. [9] in that the amplitudes are added coherently as in Ref. [7] yet an analytic form for the energy-integrated electron angular distribution is obtained. The angular distribution contains interference terms that are critical at small angles, and interference terms account for most of the collision-energy dependence observed in experiments.

Our expression for the energy-integrated electron angular distribution is developed in Sec. II. In Sec. III this expression is compared to the small-angle autoionization cross-section data of Swenson *et al.* [9] for He^+ + He at 5-, 10-, and 15-keV collision energies. The 10-keV

autoionization spectral data of Swenson *et al.* [10] are compared to the theory based on the autoionization amplitude of Refs. [8, 7]. The results are discussed in Sec. IV. Atomic units are used throughout except where explicitly noted otherwise.

II. THEORY

A. General theory

The emission angle-dependent autoionization amplitude of Ref. [8] including the Stark effect of Ref. [7] is given by

$$A_j = \mathcal{S}_j\,\Gamma\left[1 - i\frac{Z}{v'}\right]\exp\left[\pi\frac{Z}{2v'}\right] \times \int_0^\infty \exp\left[i\left(E - E_j + i\frac{\Gamma_j}{2}\right)t\right] t^{i\frac{z}{v}} \times {}_1F_1\left(i\frac{Z}{v'}, 1; i(v'v - \mathbf{v}'\cdot\mathbf{v})t\right) dt, \quad (2.1)$$

where Z is the projectile charge, $\mathbf{v}$ is the velocity of the projectile, $\mathbf{v}_e$ is the velocity of the autoionized electron, $\mathbf{v}' = \mathbf{v}_e - \mathbf{v}$ is the velocity of the electron relative to the projectile, E_j is the resonant energy of the autoionizing state, Γ_j is the linewidth of the state, t is the time after the collision, and $\mathcal{S}_j$ is the inherent angular variation and phase of the amplitude that depends on the angular momentum of state j combined with the Stark effect (see Appendix for details). One should note that the time integral is evaluated analytically in Ref. [8], and this form will be used later for spectral calculations.

For several overlapping lines the amplitude is the sum of individual amplitudes multiplied by complex constants a_j representing the population and relative phase of each state. The electron angle-dependent transition rate $w(\Omega)$ is obtained by integrating the squared amplitude over electron energy

$$w(\Omega) = \int_0^\infty \sum_{i,j} a_i^* a_j A_i^* A_j\, dE. \quad (2.2)$$

This transition rate $w(\Omega)$ is proportional to the cross section $\frac{d\sigma}{d\Omega}$.

The order of the sum and integral over energy can be exchanged because the integral converges, and the constants $a_i^* a_j$ taken outside the integral because they do not depend on the energy. Since the amplitude A_j is zero for $E < 0$, the lower limit can be extended to $-\infty$ without serious error. Further, the resonant line amplitude is well localized near the resonant energies, therefore the peaking approximation $v_e = v_{\rm ave} = \sqrt{2E_{\rm ave}}$, $E_{\rm ave} = (E_i + E_j)/2$ is also made. Now only a common factor that depends explicitly on energy, $\exp[iEt - iEt']$, remains under the energy integral. The integral of $\exp[iEt - iEt']$ over E just gives $2\pi\delta(t - t')$, and Eq. (2.2) becomes

$$w(\Omega) = \sum_{i,j} a_i^* a_j \mathcal{S}_i^* \mathcal{S}_j \left|\Gamma[1 - iZ/v'_{\rm ave}]\right|^2 e^{\pi\frac{Z}{v'_{\rm ave}}} \times \int_0^\infty \exp\left[\left(i(E_i - E_j) - \frac{\Gamma_j + \Gamma_i}{2}\right)t\right] \times {}_1F_1\left(i\frac{Z}{v'_{\rm ave}}; 1; id_{\rm ave}t\right) \times {}_1F_1\left(-i\frac{Z}{v'_{\rm ave}}; 1; -id_{\rm ave}t\right) dt, \quad (2.3)$$

where

$$d_{\rm ave} = v'_{\rm ave}v - \mathbf{v}'_{\rm ave}\cdot\mathbf{v}. \quad (2.4)$$

The remaining integral over time involving two confluent hypergeometric functions is evaluated analytically using Eq. (7.6221) of Gradshteyn and Ryzhik [14] to obtain

$$w(\Omega) = \sum_{i,j} w_{ij}(\Omega), \quad (2.5)$$

where

$$w_{ij}(\Omega) = a_i^* a_j \mathcal{S}_i^* \mathcal{S}_j \frac{\pi Z\, e^{\pi Z/v'_{\rm ave}}}{v'_{\rm ave}\sinh(\pi Z/v'_{\rm ave})}\frac{1}{g_{ij}} \times \left[\frac{g_{ij} + id_{\rm ave}}{g_{ij} - id_{\rm ave}}\right]^{\frac{iZ}{v'_{\rm ave}}} \times {}_2F_1\left(i\frac{Z}{v'_{\rm ave}}, -i\frac{Z}{v'_{\rm ave}}; 1; \frac{1}{1 + \left(\frac{g_{ij}}{d_{\rm ave}}\right)^2}\right), \quad (2.6)$$

$$g_{ij} = i\,(E_j - E_i) + \frac{\Gamma_j + \Gamma_i}{2}, \quad (2.7)$$

and where ${}_2F_1(a, b, c; z)$ is a Gaussian hypergeometric function. The quantities $w_{ij}(\Omega)$ are defined for convenience, and have the structure of a density-matrix element.

When $i = j$, the expression for $w_{jj}(\Omega)$ simplifies to

$$w_{jj}(\Omega) = |a_j|^2\frac{|\mathcal{S}_j|^2}{\Gamma_j}\frac{\pi Z}{v'_j\sinh(\pi Z/v'_j)} \times \exp\left\{\frac{Z}{v'_j}\left[\pi - 2\arctan\left(\frac{d_j}{\Gamma_j}\right)\right]\right\} \times {}_2F_1\left(i\frac{Z}{v'_j}, -i\frac{Z}{v'_j}; 1; \frac{1}{1 + \left(\frac{\Gamma_j}{d_j}\right)^2}\right), \quad (2.8)$$

where $d_j = v'_j v - \mathbf{v}'_j\cdot\mathbf{v}$ and $v_j = \sqrt{2E_j}$. This $w_{jj}(\Omega)$ is the transition rate for a single isolated line.

The cross terms in Eq. (2.5) can be grouped to combine terms that are complex conjugates of each other, $w_{ij}(\Omega)$ and $w_{ji}(\Omega)$, by taking twice the real part of $w_{ij}(\Omega)$,

$$\tilde{w}_{\{ij\}}(\Omega)=\frac{\pi Z\, e^{\pi Z/v'_{\rm ave}}}{v'_{\rm ave}\sinh(\pi Z/v'_{\rm ave})} \times 2\,\mathrm{Re}\left\{ a_i^* a_j \mathcal{S}_i^* \mathcal{S}_j \frac{1}{g_{ij}} \left[\frac{g_{ij}+id_{\rm ave}}{g_{ij}-id_{\rm ave}}\right]^{\frac{iZ}{v'_{\rm ave}}} \times {}_2F_1\left(i\frac{Z}{v'_{\rm ave}}, -i\frac{Z}{v'_{\rm ave}}; \frac{1}{1+\left(\frac{g_{ij}}{d_{\rm ave}}\right)^2}\right)\right\}. \tag{2.9}$$

One should note that this expression for the interference terms has no physical meaning outside the sum over states that includes $w_{jj}(\Omega)$ and $w_{ii}(\Omega)$. Because of the term $1/(g_{ij}-id_{\rm ave})^{iZ/v'_{\rm ave}}$ in $\tilde{w}_{\{ij\}}(\Omega)$, one would expect an extremum in the interference term at the angle where $(E_j-E_i)-d_{\rm ave}=0$, i.e., at

$$\cos(\theta)=\frac{-(E_j-E_i)}{vv_{\rm ave}}+\sqrt{1+\frac{2(E_j-E_i)}{v_{\rm ave}^2}}, \tag{2.10}$$

but for some values of the phases this extremum may be difficult to detect. It should also be noted that for large differences in energy between the resonance states, $E_j-E_i\to\infty$, the interference terms $\tilde{w}_{\{ij\}}(\Omega)$ vanish, thus expression (2.5) becomes a sum of terms representing isolated lines.

The angular-dependent transition probability is now written as

$$w(\Omega)=\sum_j w_{jj}(\Omega)+\sum_{\substack{i,j\\ i<j}}\tilde{w}_{\{ij\}}(\Omega). \tag{2.11}$$

B. Limiting forms

For the single isolated line at large angles where $d_j\gg\Gamma_j$, the argument of the hypergeometric function in Eq. (2.8) is nearly unity so that the hypergeometric function can be approximated by $\sinh(\pi Z/v'_j)/(\pi Z/v'_j)$, and $\arctan(d_j/\Gamma_j)\approx\pi/2$. Then

$$w_{jj}(\Omega)=|a_j|^2\frac{|\mathcal{S}_j|^2}{\Gamma_j}, \tag{2.12}$$

which is the transition probability one obtains from a Lorentzian, or a Devdariani-type [4] line shape without Coulomb focusing of the autoionization electrons. This expression depends upon the population of the state $|a_j|^2$ and its angular momentum through $|\mathcal{S}_j|^2$.

For an isolated line in the forward direction where $d_j\ll\Gamma_j$, so that the hypergeometric function in Eq. (2.8) is approximately unity and the $\arctan\left(\frac{d_j}{\Gamma_j}\right)\approx 0$, one has

$$w_{jj}(\Omega)=|a_j|^2\frac{|\mathcal{S}_j|^2}{\Gamma_j}\frac{\pi Z\,\exp\left[\frac{Z}{v'_j}\pi\right]}{v'_j\sinh(\pi Z/v'_j)}, \tag{2.13}$$

which is the absolute value squared of the Coulomb normalization factor for an electron in the field of the projectile of charge Z multiplied by the transition probability obtained at large angles.

For the interference terms $\tilde{w}_{\{ij\}}(\Omega)$ the angular limits are similar. In the forward direction where $d_{\rm ave}\ll g_{ij}$, the hypergeometric function in Eq. (2.9) is approximately unity, and $[(g_{ij}+id_{\rm ave})/(g_{ij}-id_{\rm ave})]\approx 1$. Thus, for small angles

$$\tilde{w}_{\{ij\}}(\Omega)=\frac{\pi Z\,\exp\left[\frac{Z}{v'_{\rm ave}}\pi\right]}{v'_{\rm ave}\sinh(\pi Z/v'_{\rm ave})}2\,\mathrm{Re}\left\{a_i^* a_j \mathcal{S}_i^* \mathcal{S}_j\frac{1}{g_{ij}}\right\}. \tag{2.14}$$

Again one sees the Coulomb normalization factor squared but here it is multiplied by the phase-dependent expression $2\,\mathrm{Re}\{a_i^* a_j \mathcal{S}_i^* \mathcal{S}_j/g_{ij}\}$. Since g_{ij} involves E_i-E_j, which is often significantly larger than $(\Gamma_i+\Gamma_j)/2$, the contribution to the complete transition probability of Eq. (2.11) will be smaller than the contributions from the single resonance terms. But these contributions cannot be ignored at 0° because they can be either positive or negative, and, as will be seen, can have a significant effect on the cross section at small angles.

At large angles a good approximation for the interference terms is difficult to determine because E_i-E_j can be large; but in such cases the interference terms would be small and ignorable at all angles. However, if E_i-E_j is small so that $d_{\rm ave}\gg g_{ij}$ one can approximate the hypergeometric function in Eq. (2.9) with $\sinh(\pi Z/v'_{\rm ave})/(\pi Z/v'_{\rm ave})$, and $[(g_{ij}+id_{\rm ave})/(g_{ij}-id_{\rm ave})]^{(iZ/v'_{\rm ave})}\approx e^{-\pi Z/v'_{\rm ave}}$ giving

$$\tilde{w}_{\{ij\}}(\Omega)=2\mathrm{Re}\left\{a_i^* a_j \mathcal{S}_i^* \mathcal{S}_j\frac{1}{g_{ij}}\right\}, \tag{2.15}$$

which is a smaller contribution to the complete transition probability than the single resonance terms because of E_i-E_j in g_{ij}.

III. APPLICATION

In order to apply the transition probability of Eq. (2.11) to data of Swenson *et al.* [9] for the cross-section ratios of autoionization electrons emitted in 5-, 10-, and 15-keV $He^+ + He$ for $0°\le\theta\le 30°$, the relative population and phase of each state must be determined. The populations and phases were determined by fitting the autoionization spectra data of Swenson *et al.* [10] for 10-keV $He^+ + He$ at small scattering angles with the following coherent sum of resonant amplitudes

$$w(\Omega,E)=\left|\sum_j a_j A_j\right|^2, \tag{3.1}$$

where A_j is given by Eq. (2.1) [the integral over time can be evaluated analytically, see Ref. [8], Eq. (3.6)], and $a_j = c_j e^{i\chi_j}$. The population c_j and phase χ_j of each state is treated as a fitting parameter.

For 10-keV He^+ + He and $\theta \leq 10°$ the only significant states are the m=0 sublevels of $(2s^2)\,^1S$, $(2p^2)\,^1D$, $(2s2p)\,^1P$, with resonant energies $E_j = 1.224$, 1.297, 1.307, and line widths $\Gamma_j = 5.07 \times 10^{-3}$, 2.65×10^{-3}, 1.40×10^{-3}, respectively. Since our interest is in the relative population and phase of the states the parameters of one state can be set arbitrarily. We chose to set $c_{1_P} = 1$ and $\chi_{1_P} = 0$ while the ^1S and ^1D parameters are adjusted to fit the data. The fitted parameters are listed in Table I. The spectra were calculated at 0°, 5°, and 10° keeping the parameters the same at all angles and convoluting with a Gaussian energy resolution with a [full width at half maximum (FWHM)] of 0.3 eV. The results are shown in Fig. 1 where the different angular spectra are normalized to a constant maximum intensity as was the experimental data taken from Ref. [10]. Unpublished experimental autoionization spectra data were obtained from Meyer [11], for 5-keV He^+ + He at 0° and 15-keV He^+ + He at 0°. These spectra were fitted in the same manner as the 10-keV data, and the results of the calculations are shown in Fig. 2. The parameters used are listed in Table I.

Reference [9] gives the cross-section ratio R,

$$R = \frac{d\sigma_{\text{target}}(\theta)}{d\Omega} \Big/ \frac{d\sigma_{\text{projectile}}(\theta)}{d\Omega} . \tag{3.2}$$

Since the excitation probabilities for the target are roughly the same as the capture probabilities for the projectile at the energy we are considering here, as can be seen in the data of Bordenave-Montesquieu, Glaeizes, and Benoit-Cattin [12], the projectile autoionization at a laboratory angle of θ can be approximated by the target autoionization in the backward direction at the kinematically shifted angle,

$$\theta' = \arcsin\left\{\left[\frac{v\cos\theta}{v_e} - \sqrt{1 - \left(\frac{v\sin\theta}{v_e}\right)^2}\right]\sin\theta\right\} . \tag{3.3}$$

The fitted parameters of Table I were used to calculate the transition-probability ratio

$$R = \frac{w(\theta)}{w(\theta')} . \tag{3.4}$$

Since the experimental data are cross-section ratios, the proportionality constants needed to convert the transition probabilities into cross sections will cancel, and the ratio of transition probabilities equals the cross-section ratio R.

The parameters in Table I were used to calculate the transition-probability ratios R of Eq. (3.4) using Eq. (2.11) for 5-, 10-, and 15-keV He^+ + He for $0° \leq \theta \leq 30°$. This ratio is convoluted with a Gaussian angular resolution of 2.7°, to represent the 2.7° angular acceptance of the analyzer reported in the experimental data

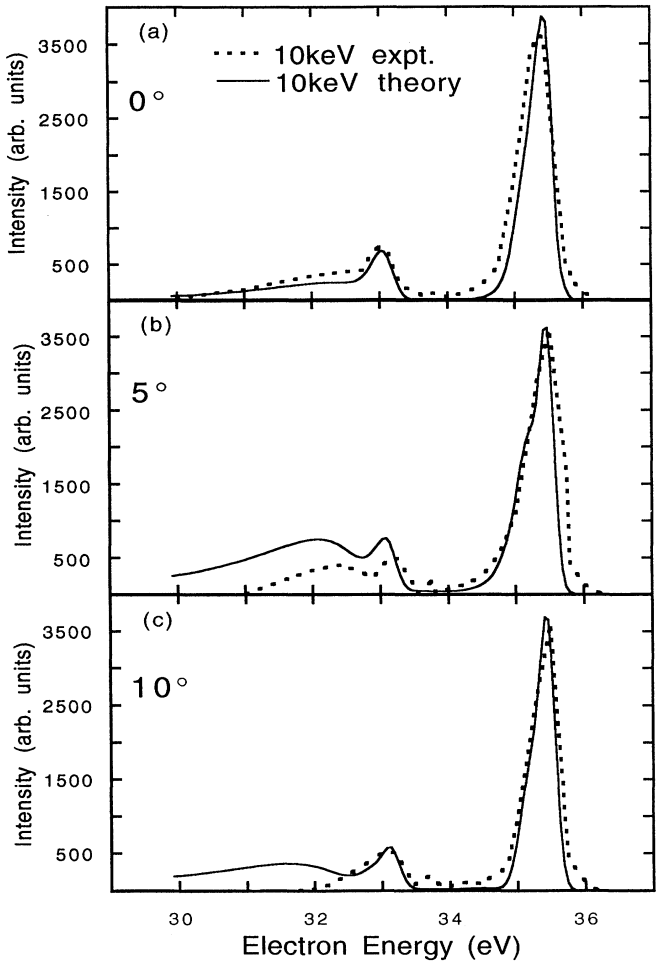

FIG. 1. Autoionization electron spectra calculated with this theory for 10-keV He^+ + He shown with the experimental data of Ref. [10]. (a) , (b), and (c) are the spectra at 0°, 5°, and 10°, respectively. The calculations use the coherent sum of perturbed autoionization amplitudes given by Eq. (3.1), with the fitted parameters $a_j = c_j e^{i\chi_j}$ of Table I. The spectra were normalized to a constant magnitude to match the normalization of the experimental data.

TABLE I. Fitted parameters for spectral and cross-section ratio calculations for He^+ + He at 5-, 10-, 15-keV collision energies. $|c_j|^2$ and χ_j are the relative population and phase, respectively, of the state j.

	5 keV	10 keV	15 keV
c_{1_S}	1.0	1.0	0.9
χ_{1_S}	1.1π	1.3π	1.2π
c_{1_D}	0.7	0.2	0.5
χ_{1_D}	1.7π	1.5π	1.2π
c_{1_P}	1.0	1.0	1.0
χ_{1_P}	0	0	0

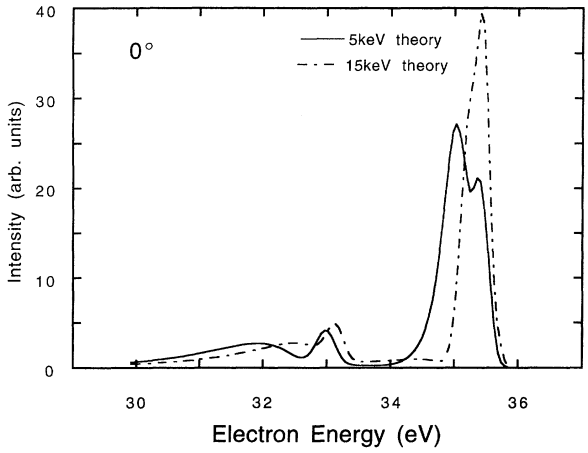

FIG. 2. Autoionization electron spectra calculated with this theory for 5- and 15-keV $He^+ + He$ at 0°. The calculations use the coherent sum of perturbed autoionization amplitudes given by Eq. (3.1), with the fitted parameters $a_j = c_j e^{i\chi_j}$ of Table I. Each spectrum was normalized by the sum of its state populations $1/\sum_j |a_j|^2$.

[9]. The results are shown with the data of Ref. [9] in Fig. 3(a). Figure 3(b) shows the cross-section ratio plots for 5, 10, and 15 keV using the same parameter sets as in Fig. 3(a), except that in these calculations the interference terms $\tilde{w}_{\{ij\}}(\Omega)$ of Eq. (2.11) have been removed from the calculation.

In principle the scattering of the projectile should be taken into account because the theory used here measures the angle relative to the trajectory of the projectile ion; thus, 0° is along the scattered direction of the projectile. However, the data of Bordenave-Montesquieu and Dagnac [13] show that this scattering is small (< 2° for 5-keV $He^+ + He$, < 1° for 15-keV $He^+ + He$), and since the cross section is not divergent at 0° convoluting with a distribution to represent this scattering would change the calculations only slightly. Likewise, the 0.5° angular divergence of the projectile beam reported in Ref. [9] would have minimal impact on the calculations performed in this paper. Thus these two effects were not taken into account, but if they were included may lead to a slightly better fit at 0° for the cross-section ratios.

IV. DISCUSSION

The cross-section ratio calculation for 10 keV [see Fig. 3(a)] is in good agreement with experiment; however, the spectral fits for 10 keV [see Fig. 1] show some disagreement. At 5° the ^1S line and its low-energy tail are almost a factor of 1.6 too large. At 10° the low-energy tail below 32.5 eV is absent in the measurement but present in the theory. These disagreements are comparable to those of the Coulomb path semiclassical model of Swenson *et al.* [10], where at 5° the ^1S line is nearly a factor of 2 too small and at 10° the peak region around 33 eV is too broad. Qualitatively the Coulomb trajectory model appears better at 10°. One possible explanation

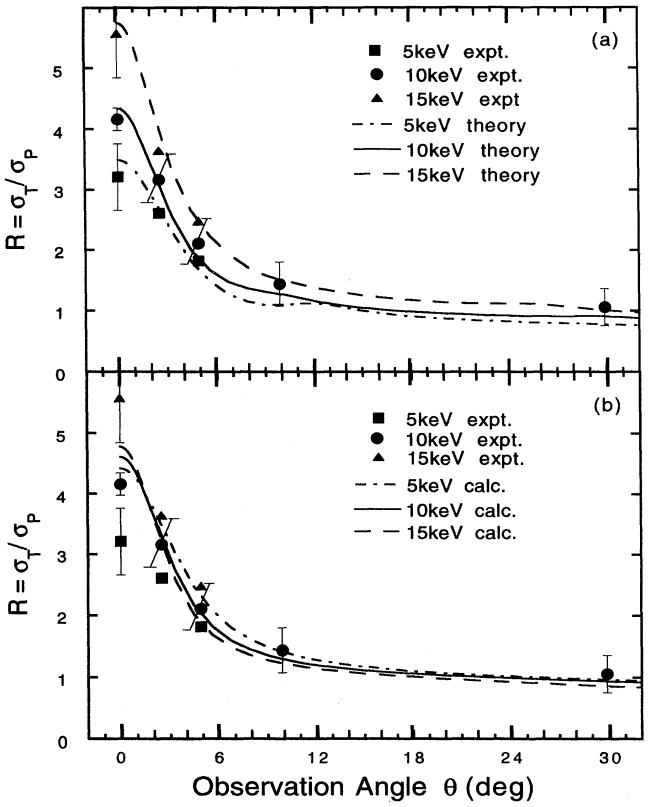

FIG. 3. (a) Cross-section ratio $R = \sigma_{\text{target}}/\sigma_{\text{projectile}}$ calculations for 5-, 10-, and 15-keV $He^+ + He$ using Eq. (3.4) shown with the experimental data of Ref. [9]. (b) Same as (a) except for the omission of interference terms in the calculation.

for the calculated 10°, 10-keV ^1S tail that does not appear in the data is the background subtraction in the 10° experimental data. Because the ^1S line's low-energy tail is so broad at 10°, and occurs in the region where the background is the largest, it might have been subtracted as part of the background.

The failure of the amplitude of Ref. [8] to match the spectral data at all angles stems from the low-energy tail of the ^1D-^1P peak, where autoionization occurs at small internuclear distances, and where good approximations to both the binding and Stark effects are not readily available. Agreement between theory and experiment in this region was improved with the Stark-mixing modifications to the amplitude described in Ref. [7] and contained in $\mathcal{S}_j$ of Eq. (2.1), but the basic model of Ref. [8] appears inadequate for very small internuclear distances where the autoionization observed in the tails of the peaks occurs. As a rough estimate, the ^1D-^1P tail region around the ^1S peak (near 33 eV in the spectra) corresponds to emission at an internuclear separation of $\sim$10 a.u. where the Stark corrections are not well represented in $\mathcal{S}_j$; thus discrepancies in this region are not surprising. Since this tail region does not contribute much to the cross section integrated over energy, Eq. (2.11) for the cross section of overlapping lines is a good approximation, as shown by

the ratios in Fig. 3(a). One should also note that the data of Ref. [12] provide information on the populations of the three states used here for 10- and 15-keV He^+ + He; these data give relative populations of 0.96, 0.17, and 1.0 for 10 keV and 0.84, 0.40, and 1.0 for 15 keV for the ^1S, ^1D, and ^1P states, respectively. These values are to be compared with the $|c_j|^2$ parameters used in the calculations of this work. These data are in reasonable agreement with the fitted relative populations given by the squares of the c_j parameters listed in Table I except for the ^1D, $m = 0$ populations; but since these data were taken at larger angles ($\theta \geq 20°$) where the ^1D, $|m| = 2$ state is by far the dominant contribution to the cross section, the ^1D, $m = 0$ population would have an uncertainty comparable to the discrepancy of the fitted parameter and the measured value.

When comparing Figs. 3(a) and 3(b) it is important to observe that while the 10-keV cross-section ratio is altered only a small amount by the interference terms (because the fitted phases of the dominant ^1D-^1P interference term make its contribution small), the 5- and 15-keV ratios are altered dramatically by the presence of the interference terms. In fact, without the interference terms the experimental cross-section ratio data could not be matched for these energies, as is seen in Fig. 3(b).

These interference terms can also introduce some structure into the angular-dependent cross section, as can be seen in the 5-keV cross-section ratio calculation [Fig. 3(a)] near 12°. This energy and angle correspond to the extremum of the ^1D-^1P interference term described in Eq. (2.10) for 5-keV He^+ + He cross section. The other extrema are not seen in the cross-section ratio calculations because the ^1S-^1P and ^1S-^1D terms are small due to the large difference in resonance energy of the states. The 10-keV ratio shows no additional structure because the fitted phases make all interference terms small. The ^1D-^1P interference-term extremum is not observed in the 15-keV calculation because the choice of phases obscures this maximum.

V. CONCLUSION

The perturbed autoionization amplitude of Refs. [7, 8] was used to construct a squared coherent sum of states that represents the postcollision autoionization electrons in low-energy ion-atom collisions. This sum was analytically integrated over energy to yield the angle-dependent autoionization cross section. The most striking feature of this work is the interference terms of the transition probability, $\tilde{w}_{\{ij\}}(\Omega)$ of Eq. (2.11). These terms are necessary for describing the collision-energy dependence of experimentally measured cross-section ratios near 0°. The sign and magnitude of these terms is very dependent on the relative phase of the states involved. Thus it is necessary to have accurate phase information about the states near 0° where these interference terms are most significant. This phase information can be provided by autoionization electron spectra.

The agreement of experiment and this theory is good for the autoionization cross-section ratios calculated for 5-, 10-, and 15-keV collisions of He^+ + He. The calculated spectra show some discrepancies with experiment in the low-energy tail region of the autoionization amplitude, indicating a possible breakdown of the model for very small internuclear collision distances (around 10 a.u. separation), or problems with background subtraction in the published experimental data.

These results show that the present theory gives a good description of Coulomb focusing and binding effects. It also indicates that the Stark effect plays some role.

ACKNOWLEDGMENT

Support for this research under National Science Foundation Grant No. PHY-8918713 is gratefully acknowledged.

APPENDIX: DEFINITION OF $\mathcal{S}_j$

To define the $\mathcal{S}_j$ term of Eq. (2.1), we take the following from Ref. [7]. For an autoionization state of angular momentum L and magnetic quantum number $|M|$ that is not Stark mixed with another state, we have

$$\mathcal{S}_{LM} = \gamma_{LM} = (-i)^L e^{i \arg \Gamma(L+1-i/\sqrt{2E})} \times \left[\frac{\Gamma_L}{2\pi\sqrt{2E}}\right]^{1/2} Y_L^{\bar{M}}(\Omega), \tag{A1}$$

and $Y_L^{\bar{M}} = [Y_L^{-M} + (-1)^M Y_L^M]/\sqrt{2}$ for $M \neq 0$, ($Y_L^{\bar{0}} = Y_L^0$).

For two Stark-mixed states L and L' of the same magnetic quantum number $|M|$, the expressions of Ref. [7] give

$$\mathcal{S}_{LM} = \gamma_{LM} \cos(\Lambda_{L,L',M}) - i\gamma_{L'M} \sin(\Lambda_{L',L,M}), \tag{A2}$$

$$\mathcal{S}_{L'M} = \gamma_{L'M} \cos(\Lambda_{L',L,M}) - i\gamma_{LM} \sin(\Lambda_{L,L',M}), \tag{A3}$$

where

$$\Lambda_{L,L',M} = |\beta_M| \left(\frac{\Gamma_L}{2} + i(E_L - E)\right)^2 \frac{1}{\frac{Z}{v}\left\{i\left[\frac{\Gamma_L}{2} + i(E_L - E)\right] + (E_L - E_{L'})(i\frac{Z}{v} - 1)\right\}}. \tag{A4}$$

β_M equals the dipole matrix element coupling the states LM and $L'M$, and γ_{LM} is given in Eq. (A1).

The three significant autoionizing states excited in He^+ + He in the collision-energy range 5–15 keV and scattering angles $0° \leq \theta < 15°$ are the $M = 0$ sublevels of $(2s^2)\,^1S$, $(2p^2)\,^1D$, $(2s2p)\,^1P$, with resonant energies $E_j = 1.224$, 1.297, 1.307, respectively. For these states, the ^1S is sufficiently separated in resonance energy that it does not Stark mix with the other states, so $\mathcal{S}_{^1S,0}$ is of the unmixed form given above [Eq. (A1)]. The ^1D and

^1P states do Stark mix as described above with

$$\beta_0 = \frac{-2\sqrt{3}}{1.7v^2}. \tag{A5}$$

It should be noted, as it is in Ref. [7], that this approximation of the Stark mixing maintains unitarity to within a few percent.

[1] M. Yu. Kuchiev and S. A. Sheinerman, Usp. Fiz. Nauk **158**, 353 (1989) [Sov. Phys. Usp. **32**, 569 (1989)].

[2] M. Yu. Kuchiev and S. A. Sheinerman, J. Phys. B **21**, 2027 (1988).

[3] R. B. Barker and H. W. Berry, Phys. Rev. **151**, 14 (1966).

[4] A. Z. Devdariani, V. N. Ostrovsky, and Yu. N. Sebyakin, Zh. Eksp. Teor. Fiz. **73**, 412 (1977) [Sov. Phys. JETP **46**, 215 (1977).

[5] P. Van der Straten and R. Morgenstern, J. Phys. B **19**, 1361 (1986).

[6] N. Stolterfoth, D. Brand, and M. Prost, Phys. Rev. Lett. **43**, 1654 (1979).

[7] J. E. Miraglia and J.H. Macek, Phys. Rev. A **42**, 3971 (1990).

[8] R. Barrachina and J.H. Macek, J. Phys. B **22**, 2151 (1989).

[9] J. K. Swenson, C. C. Havener, N. Stolterfoht, K. Sommer, and F. W. Meyer, Phys. Rev. Lett. **63**, 35 (1989).

[10] J. K. Swenson, J. Burgdörfer, F. W. Meyer, C. C. Havener, D. C. Gregory, and N. Stolterfoht, Phys. Rev. Lett. **66**, 417 (1991).

[11] F.W. Meyer (private communication).

[12] A. Bordenave-Montesquieu, A. Glaeizes, and P. Benoit-Cattin, Phys. Rev. A **25**, 245 (1982).

[13] D. Bordenave-Montesquieu and R. Dagnac, J. Phys. B **12**, 1233 (1979).

[14] I. S. Gradshteyn and I. Ryzhik, *Tables of Integrals, Series and Products* (Academic, London, 1977), p. 861.